HAL
open science

Rayleigh-Taylor instability experiments on the LULI2000 laser in scaled conditions for young supernova remnants

G. Rigon, A. Casner, Bruno Albertazzi, Th Michel, P. Mabey, E. Falize, J. Ballet, L. van Box Som, S. Pikuz, Y. Sakawa, et al.

HAL Id: hal-02274895

https://hal.science/hal-02274895

Submitted on 30 Aug 2019

Rayleigh-Taylor Instability experiments on the LULI2000 laser in scaled conditions for young Supernovae Remnants

G. Rigon[ORCID],[1] A. Casner,[2] B. Albertazzi,[1] Th. Michel,[1] P. Mabey,[1] E. Falize,[3] J. Ballet,[4] L. Van Box Som,[3] S. Pikuz,[5, 6] Y. Sakawa,[7] T. Sano,[7] A. Faenov,[8, 5] T. Pikuz,[8, 5] N. Ozaki,[9, 7] Y. Kuramitsu,[9] M.P. Valdivia,[10] P. Tzeferacos,[11] D. Lamb,[11] and M. Koenig[1, 9]

[1]*LULI - CNRS École Polytechnique, CEA : Université Paris-Saclay ; UPMC*
Univ Paris 06 : Sorbonne Universités - F-91128 Palaiseau cedex, FRANCE
[2]*Université de Bordeaux-CNRS-CEA, CELIA, UMR 5107, F-33405 Talence, FRANCE*
[3]*CEA-DAM, DIF, F-91297 Arpajon, FRANCE*
[4]*AIM, CEA, CNRS, Université Paris-Saclay, Université Paris Diderot,*
Sorbonne Paris Cité, F-91191 Gif-sur-Yvette, FRANCE
[5]*Joint Institute for High Temperature RAS, Moscow, 125412, RUSSIA*
[6]*National Research Nuclear University "MEPhi", Moscow, 115409, RUSSIA*
[7]*Institute of Laser Engineering, Osaka University, JAPAN*
[8]*Open and Transdisciplinary Research Initiative, Osaka Uniersity, Osaka, 565-0871, JAPAN*
[9]*Graduate School of Engineering, Osaka University, Osaka, 565-0871, JAPAN*
[10]*Department of Physics ans Astronomy, Johns Hopkins University, Baltimore, Maryland 21218, USA*
[11]*University of Chicago, Chicago, Illinois 60637, USA*

We describe a platform developed on the LULI2000 laser facility to investigate the evolution of Rayleigh-Taylor instability (RTI) in scaled conditions relevant to young Supernovae Remnant (SNR) up to 200 years. An RT unstable interface is imaged with a short-pulse laser-driven (PICO2000) x-ray source, providing an unprecedented simultaneous high spatial (24 µm) and temporal (10 ps) resolution. This experiment provides relevant data to compare with astrophysical codes, as observational data on the development of RTI at the early stage of the SNR expansion are missing. A comparison is also performed with FLASH radiative magneto-hydrodynamic simulations.

The Rayleigh-Taylor instability (RTI) [1] is a seminal hydrodynamic instability occurring at the interface between two fluids when the gradient of density is opposed to the acceleration inertial force applied on the fluid in the reference frame of the interface. The RTI occurs in many physical systems, for instance at atmospheric pressure, in the oceans or the Earth atmosphere [2], at higher pressure, in the Earth's mantle [3], or in inertial confinement fusion implosions [4] both at the ablation front [5] or in the final deceleration phase including mixing with the fuel [6]. In absence of stabilizing mechanisms such as surface tension, viscosity or magnetic fields [7], the key governing parameters are the acceleration of the fluids, g, the ratio of density through the Atwood number, $A_t = (\rho_1 - \rho_2)/(\rho_1 + \rho_2)$, and the wavelength of the interface perturbations, λ. For a single-mode perturbation, the linear growth rate of the classical RTI is defined as $\sigma = \sqrt{2\pi A_t g/\lambda}$. Despite its simple classical formulation, the RTI appears as an extremely complex problem in most cases, once the non-linear, saturation and possibly turbulent regimes are reached (see [8, 9] for an extensive review).

We concentrate hereafter on the astrophysical case of young Supernovae Remnants (SNR) interacting with the interstellar medium (ISM). The interface between those two fluids is decelerating, making it RT unstable [10]. This instability is also embedded with other hydrodynamics instabilities, such as Richtmyer-Meshkov and Kelvin-Helmholtz instabilities. Other phenomena such as the magnetic field and the radiation can affect the evolution of the SNR [11], however those only concern later time evolution. Knowing the interface dimension between SNR and ISM, and hence the compression of the shock [12, 13], also has a strong implication on cosmic rays acceleration [14]. Unfortunately this parameter can not be determined by astronomical observation as it is impeded by RTI mixing zone growth [15]. Moreover the only data available are obtained from some scarce three-dimensional simulations [16, 17], whose initial conditions are ideal and often not controlled. Actually, the seeds of the instability are usually given by the numerical noise. In the astrophysical case, the origin of the seeds is unknown, it could be due to thermal noise or coming from the exploding star. Therefore any measurement of the RTI mixing zone, as we did in our experiment will increase our confidence in SNR simulations [18], as part

of the physics involved is validated. Indeed, the principle of laboratory astrophysics [19, 20] relies on the ability to scale and mimic astrophysical problems down to Earth by using scaling laws [21, 22] implying the conservation of dimensionless numbers.

In this article, we report the results of an RTI laser experiment performed on the LULI2000 laser facility at École Polytechnique in France. We demonstrate, using scaling laws, that our experiment is similar to remnants of thermonuclear SN (type Ia SNR) such as Tycho, where tens of nanoseconds in the laboratory is equivalent to years for SNRs. Our data provide inputs on the early stage evolution of RTI in SNR, which are out of reach to astronomical instruments. Furthermore we do have a perfect control over the initial conditions, which are usually the consequences of numerical seeds in simulations [15]. Contrary to previous RTI laser plasma experiments performed over several years on larger scale facilities [23–27], the potential of short pulse driven x-ray radiography [28] allows, for the first time, one to acquire snapshots of RTI with unprecedented simultaneous spatial and temporal resolution. The RTI growth is measured until its nonlinear phase and the effect of the seed on the dynamic of RTI is quantified. One of the fundamental parameter used in RTI studies is the mixing zone (MZ) [29]. It is defined as the distance between the tip of the peak and the bottom of the bubble. In this paper, the temporal evolution of single-mode and two-mode MZ are compared. A growth of MZ by a factor of 20 was observed after 50 ns. These measurements are in agreement with the radiation-magnetohydrodynamics FLASH simulations.

The experiment was performed at the LULI2000 laser facility, and the set-up is presented in Fig 1. A multi-layer modulated target is driven by the nano2000 laser beam (500 J, 2 ω, 1.5 ns square pulse) with a supergaussian ($n = 3$) focal spot of 470 µm diameter, giving an intensity of 2×10^{14} W cm^{-2}. Our multilayer target is composed of a 10 µm parylene layer acting as an ablator, a 1 µm gold layer, acting as an x-ray shield, and a 40 µm modulated pusher (C_8H_7Br). The shock wave generated in the ablator breaks out into a 0.1 g cm^{-3} resorcinol formaldehyde ($C_{15}H_{12}O_4$) foam. The foam density is more than ten times lower than the pusher (1.3 g cm^{-3}) inducing the development of the RTI at the interface, due to its deceleration. In order to obtain relevant data the initial conditions (pre-shock) has to be known. Therefore the gold layer prevents x-rays produced by the coronal plasma to modify the initial temperature of the foam and pusher.

The position and shape of the interface are diagnosed using a side-on x-ray radiography in a point projection scheme. The x-ray source is generated with the pico2000 laser beam (55 J on target, 1 ω, ~10 ps) irradiating a 25 µm titanium wire. The radiography is performed on the orthogonal axis to the wave vector of the modulation. The radiography was performed in a bottom-up geome-

try in order to reduce noise due to relativistic electrons [28] on the detector (an imaging plate - IP). The titanium wire emits in principle x-ray centered on the K_α line at 4.5 keV, but has a strong component of hard x-rays due to bremsstrahlung emission. Thanks to the shortness of the laser pulse (10 ps) the final spatial resolution comes only from the source size and geometry as opposed to the framing camera case, where time integration also plays a role. In all present published papers on RTI using laser driven x-ray sources actual spatial resolution cannot be lower than 40 µm due to motion blurring [30]. In our experiment, a resolution of 24 µm was measured by imaging gold grids (300, 600 and 1000 lines per inch) at target position (Fig. 2). This high resolution is almost unprecedented, as there is no motion blurring in comparison to more classical set-ups (such as the coupling of a pinhole and a framing camera).

The contrast between the pusher and the foam was enhanced by doping the pusher with a high Z material (Br, 44 % in mass). Combine with the density difference of the two media, it ensures a high contrast allowing their differentiation at the interface. Contrary to experiments performed with framing cameras [23–27], each pico2000 shot corresponds to one snapshot of the evolving RTI. Therefore, to ensure the reproducibility of the experiment and study the effect of the seeds on the RTI, precise control of the initial conditions is required [27]. In our targets, a pre-imposed two-dimensional modulation was mechanically pressed on the CHBr layer, such that its interface is defined by the equation $h_z(x, y) = \sum_n a_{0,n} \sin(2\pi x/\lambda_n)$, with $a_{0,n} = 10$ µm. The modulation profiles were characterized by optical interferometry. The large initial amplitude allows one to prevail over any other perturbations to grow significantly during the RTI, thus leading to a reproducible problem. The use of a phase plate (HPP) produces a nearly flat focal spot without any large hot spots, thus limiting the effect of the possible laser imprinting on the RTI. Moreover if any imprint seeds remain, they would have annealed during the shock propagation into the thick target [31]. Two different initial pattern were investigated: a single-mode with $\lambda = 120$ µm and a two-mode modulation with $\lambda_1 = 70$ µm and $\lambda_2 = 130$ µm. A simple consideration on the linear development of the instability leads to the prediction that the 70 µm wavelength should grow faster, all the others parameters being initially similar.

Except for the pre-imposed perturbation, this experiment describes a system similar to a SNR interacting with the ISM. In Table I, we compare typical parameters, relevant to the SN evolution and to the RTI development, either estimated from FLASH simulations reproducing the experiment or estimated from the astrophysical cases of SN Ia such as SN 1572 (Tycho). For this experiment to be scalable the Euler and Atwood
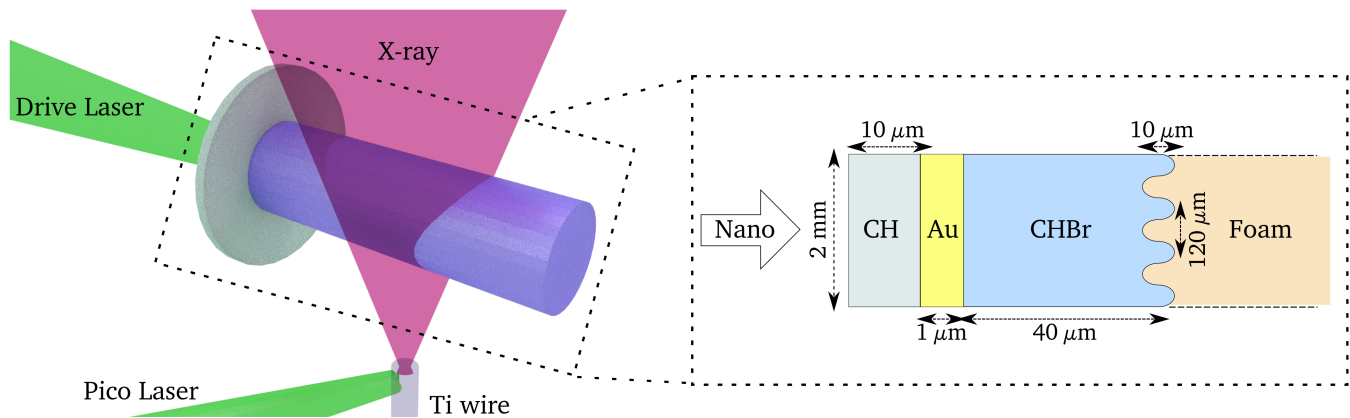
FIG. 1. Diagram of the experimental setup (left) and details of the multi-layer target (right). The target is composed of a CH ablator, a gold layer, a CHBr pusher, and a CH foam filled tube.
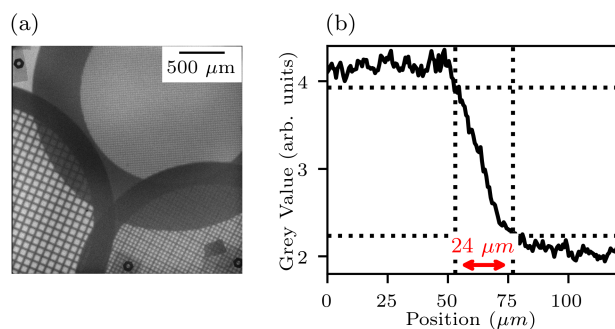

FIG. 2. (a): Radiograph of three gold grids (300, 600 and 1000 lines per inch) at target position. (b): Lineout of the border of a grid. A static resolution of 24 µm is measured (see red (light gray) arrow).

	SN Ia (100 years)	Experiment (t = 30 ns)
Length (cm)	1.3×10^{18}	5×10^{-2}
Velocity ($km\,s^{-1}$)	4000	15
Density ($g\,cm^{-3}$)	7.3×10^{-23}	0.4
Euler	$\lesssim 1$	$\sim 0.6 - 1.1$
Atwood	$0.5 - 0.7$	0.86 (initially)
		0.34 (after 50 ns)
Péclet	$\gg 1$ ($\sim 10^{12}$)	2×10^5
t_{rad}/t_{hydro}	$\gg 1$	1500

TABLE I. Scaling between the laboratory and Tycho SNR astrophysical system. The experimental numbers were obtained from FLASH simulations reproducing experimental observables.

numbers, which describe the RTI dynamics, are critical so they were made comparable. The Euler number is the ratio of thermal and dynamic pressures. The Atwood number depends on the two media initial densities, and strongly influence the RTI growth rate. In our experiment according to Table I numbers, we can expect that the hydrodynamic of the pusher-foam interface is similar to the interface of SNR's ejecta shocked ISM. Moreover we also observe a good agreement of the other dimensionless numbers for SNR and experiment. They are of the same order of magnitude, which is significant, since it determines which physical regimes are applied and which terms can be neglected. The high Péclet number and cooling parameter (t_{rad}/t_{hydro}), as defined in [21], ensures that the evolution of the system is predominantly advective (as opposed to radiative or conductive) as in the astrophysical case. As we consider the early phase of SNR expansion, before the transition to the Sedov-Taylor phase, radiative cooling is negligible and the approximation of adiabatic expansion of a perfect fluid is justified. According to scaling laws, 1.3×10^{18} cm in the astrophysical case corresponds to

0.05 cm in the experiment and 100 years correspond to 30 ns.

In our experiment, we were able to follow the whole dynamics of the decelerating RTI using a series of laser shots on the same targets with almost identical laser conditions. Moreover, the variation of the drive laser's energy from shot to shot can be overcome by rescaling the time axis of each shot, as performed in [29]. To this end, the time of the radiography can be rescaled by a characteristic time $\tau = (m/I_0)^{1/3}$, where m is the ablated mass supposed to be constant and I_0 is the laser intensity, which is directly proportional to the energy deposition. Since the laser temporal shape and focal spot are well controlled, only the uncertainty over the invariance of the target remains. So the time of the radiography is rescaled by a scaling factor such as $\tilde{t} = t(E/E_0)^{1/3}$, where $\tilde{t}$ is the new time, t is the radiography time in experiment, E is the measured total laser energy on target and E_0 is equal to 500 J.

Figures 3 (a) and (c) show x-ray radiographs obtained at a delay of 30 ns after the laser drive for the mono- and bi-mode cases. The opaque expanding pusher (bent and modulated part) can easily be distinguished from the
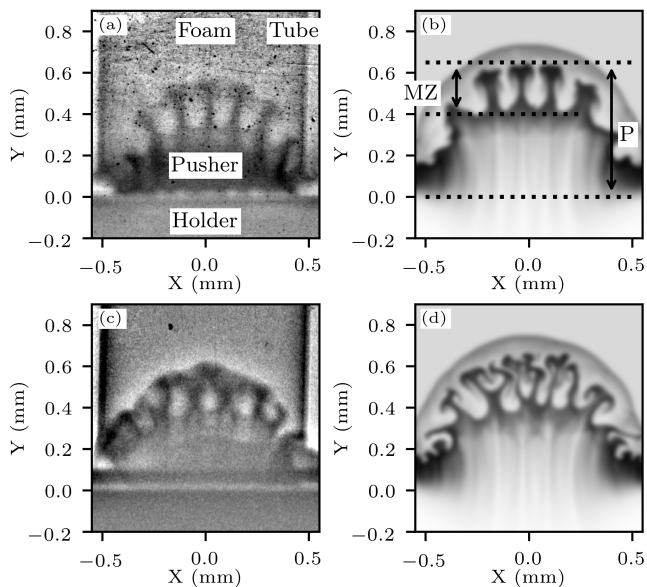
FIG. 3. Comparison of experimental (left) and synthetic (right) radiographies obtained 30 ns after laser drive. The mono-mode ((a) and (b)) and bi-mode ((c) and (d)) targets are presented. The mixing zone (MZ) is defined has the distance between peak and bubble.
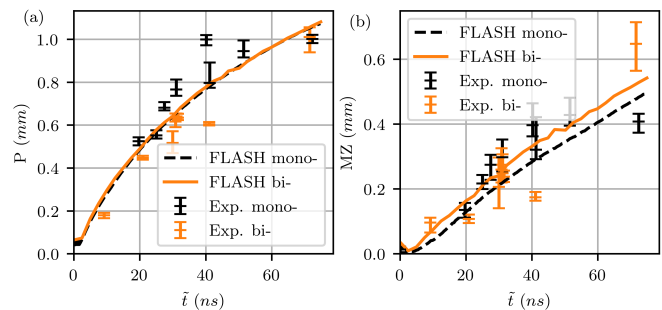

FIG. 4. Experimental interface position (a) and MZ (b) as a function of time, in both mono-mode and bi-mode cases, compared with the associated simulations. The time is rescaled by a factor of $(E/E_0)^{1/3}$ to remove the variation in drive energy from shot to shot.

foam filled tube. The edges of the tube (two parallel dark lines) and the target holder (highly contrasted part under $y = 0\,\mu m$) are also observed. The curvature of the interface between the pusher and foam is a consequence of the energy deposition. Since the focal spot has a supergaussian intensity distribution profile, a higher pressure is imposed on a 380 μm central part and decreasing at the edges. Furthermore its limited spatial expansion causes edge effects, such as rarefaction waves or radial thermal conduction, which can lead to the curvature of the shock. The materials, and interfaces, put into motion by the shock will consequently be bent. In these snapshots, the observed RTI is in its non-linear phase, indicated by the presence of the Kelvin-Helmholtz (KH) roll-up at the end of the spike. Furthermore a slight interaction between modes, only possible in the non-linear phase, is clearly visible in the bi-mode case (Fig. 3 (c)).

A side-by-side comparison between the experimental radiographs and postprocessed simulations is also shown in Fig. 3. The simulations were performed with the FLASH code developed at the Flash Center (University of Chicago) [32, 33]. This adaptive mesh refinement code was used in a two-dimensional Cartesian geometry, with 40 radiation groups. The synthetic radiographs are obtained from a post-processing developed at LULI, taking into account the density and its associated cold absorption coefficients (Henke) for the different species (pusher, foam, tube...) [34]. Here we assume a monochromatic x-ray source, a simple approximation as hard component due to bremsstrahlung is expected with short pulse laser

generated sources. In both radiographs (experiment and postprocessed simulation), the pusher-foam interfaces are similar in morphology. The RTI has also reached the non-linear stage in the simulations, as evidenced by the presence of the KH roll-up. The main difference between experiment and simulation is the observation of the shock in the foam, which is not present in the experimental case. This difference can be explained by the combination of two main processes not taken into account in our simulations. The first is the presence of a higher energy photon component, whereas the simulation is performed with a mono-energetic source. Higher energy photon are less absorbed, thus the resulting image has a lower contrast (the contrast drops from 78 % at 4.5 keV to 10 % at 10 keV). The second process is linked to three-dimensional effects not taken into account in the simulation. As the curvature of the shock wave in the direction of the radiography is not reproduced, the thickness of the shock is overestimated. This effect could be modeled if the simulation was done in cylindrical geometry around the velocity direction. However such symmetry is incompatible with the linear geometry of the modulation.

The weakly non-linear phase observed at 30 ns after laser shot is coherent with astrophysical simulations presented in Fig. 9 of Ref. [15]. Indeed the RTI corresponding to 100 years after the SN explosion should be in a weakly non-linear phase according to those simulations.

During this experiment, the dynamics of the RTI was reconstructed up to 70 ns after the main laser pulse using a full set of shots. The MZ, a good indicator of the RTI growth, was determined. Another important parameter we measured is the position of the interface between the ablator and the pusher, P, that governs all the dynamics. As the Atwood number was fixed for both type of targets and the interface's acceleration was measured to be the same (see 4 (a)), the linear growth rate σ depends only on the wavelength of the perturbation. However the difference between mono-mode and bi-mode cases was measured to be negligible.

Figure 4 shows a comparison between the measured and simulated interface position, P, and MZ growth. The error bars in figure 4 are given by the uncertainty of the interface position (peaks or bubbles), they can vary from shot to shot. P is well reproduced by the FLASH simulation and the deceleration is decreasing with time in a range from $1\,\mathrm{km\,s^{-1}\,ns^{-1}}$ to $0.2\,\mathrm{km\,s^{-1}\,ns^{-1}}$. As observed in figure 4 (a), the dynamics of the interface is the same for both mono-mode and bi-mode cases. The simulated growth of MZ differs. This is due to the presence of the lower wavelength ($70\,\mu m$) in the bi-mode case, that induces a higher growth rate σ. Despite the good reproduction of the interface position by the code, a difference appears when comparing the MZ growth with the experiment (see 4 (b)). The mono-mode MZ growth in experiment is more important than the bi-mode one. As a consequence the MZ evolution is well simulated in the bi-mode case, but under-estimated in the mono-mode case. This underestimation was already observed in [35] and attributed to an overestimation of the dilution. A difference in morphology between simulation and experiment appear for both targets at later time ($70\,\mathrm{ns}$). In simulation, non-linear and diffusive effects lead to the deformation of the spikes, they are bent, the tip is hollowed out, and the mushroom cap expanded laterally. In experiment the spikes become twisted and the cap seems to disappear. This is mainly due to the stretching of the spikes leading to a loss in contrast (the mass is more diffuse).

In summary, an experiment was performed on LULI2000 in order to study the evolution of RTI in deceleration phase until its early non-linear stage. This experiment is equivalent to the early phase of SNR expansion (before the Sedov-Taylor phase) according to the scaling laws. The non-linear phase attained in our experiment corresponds to the one predicted by astrophysicists. The platform we developed allows one to produce accurate data for the RTI of young SNR that will constrain the astrophysical simulations, which lack observational data on the early stages of SNR expansion (100 years). In particular, the ability offered by petawatt transverse radiography is appealing, especially if coupled in the near future with lithium fluoride crystal detectors that provide micrometric spatial resolution [36, 37]. The growth of the MZ of the RTI seems to be weakly affected by the initial perturbation of the interface at early time, but differences appear at later time. Some results of our experiment are accurately simulated, using the FLASH code. However we pointed out some discrepancy in MZ growth that provides inputs to improve the FLASH code and more generally astrophysical hydrodynamic codes. The similarity to the astrophysical case will be improved using 3D initial perturbations or scaled tailored foam density profiles fabricated with additive manufacturing technology [38]. This experimental platform paves the

way for future experiments on megajoule facilities with high power backlighting beams, such as NIF-ARC [39] and LMJ-PETAL [40, 41].

[1] H. Kull, Physics Reports **206**, 197 (1991).
[2] M. Kelley, G. Haerendel, H. Kappler, A. Valenzuela, B. Balsley, D. A. Carter, W. L. Ecklund, C. Carlson, B. Häusler, and R. Torbert, Geophysical Research Letters **3**, 448 (1976).
[3] C. P. Conrad and P. Molnar, Geophys. J. Int. (1997).
[4] R. D. Petrasso, Nature **367**, 217 (1994).
[5] A. Casner, L. Masse, B. Delorme, D. Martinez, G. Huser, D. Galmiche, S. Liberatore, I. Igumenshchev, M. Olazabal-Loum, P. Nicola, J. Breil, D. T. Michel, D. Froula, W. Seka, G. Riazuelo, S. Fujioka, A. Sunahara, M. Grech, C. Chicanne, M. Theobald, N. Borisenko, A. Orekhov, V. T. Tikhonchuk, B. Remington, V. N. Goncharov, and V. A. Smalyuk, Physics of Plasmas **21**, 122702 (2014), https://doi.org/10.1063/1.4903331.
[6] D. S. Clark and M. Tabak, Phys. Rev. E **72**, 056308 (2005).
[7] S. Chandrasekhar, *Hydrodynamic and hydromagnetic stability* (Dover publications, 1970).
[8] Y. Zhou, Physics Reports **720-722**, 1 (2017).
[9] Y. Zhou, Physics Reports **723-725**, 1 (2017).
[10] R. Chevalier and R. Klein, The Astrophysical Journal **219**, 994 (1978).
[11] J. P. Ostriker and C. F. McKee, Rev. Mod. Phys. **60**, 1 (1988).
[12] J. M. Blondin and D. C. Ellison, The Astrophysical Journal **560**, 244 (2001).
[13] J. S. Warren, J. P. Hughes, C. Badenes, P. Ghavamian, C. F. McKee, D. Moffett, P. P. Plucinsky, C. Rakowski, E. Reynoso, and P. Slane, The Astrophysical Journal **634**, 376 (2005).
[14] K. A. Eriksen, J. P. Hughes, C. Badenes, R. Fesen, P. Ghavamian, D. Moffett, P. P. Plucinksy, C. E. Rakowski, E. M. Reynoso, and P. Slane, The Astro-

physical Journal **728**, L28 (2011), arXiv:1101.1454 [astro-ph.HE].

[15] F. Fraschetti, R. Teyssier, J. Ballet, and A. Decourchelle, Astronomy and Astrophysics **515**, A104 (2010).

[16] D. C. Warren and J. M. Blondin, Monthly Notices of the Royal Astronomical Society **429**, 3099 (2013).

[17] J. Fang, H. Yu, and L. Zhang, Monthly Notices of the Royal Astronomical Society **474**, 2544 (2018).

[18] G. Ferrand, A. Decourchelle, J. Ballet, and F. Teyssier, R.and Fraschetti, Astronomy and Astrophysics **509**, L10 (2010).

[19] B. A. Remington, R. P. Drake, and D. D. Ryutov, Rev. Mod. Phys. **78**, 755 (2006).

[20] D. Savin, N. Brickhouse, J. Cowan, R. Drake, S. Federman, G. Ferland, A. Frank, M. Gudipati, W. Haxton, E. Herbst, *et al.*, Reports on Progress in Physics **75**, 036901 (2012).

[21] D. Ryutov, R. P. Drake, J. Kane, E. Liang, B. A. Remington, and W. M. Wood-Vasey, Astrophysical Journal **518**, 821 (1999).

[22] E. Falize, C. Michaut, and S. Bouquet, ApJ **730**, 96 (2011).

[23] R. P. Drake, Journal of Geophysical Research: Space Physics **104**, 14505 (1999).

[24] H. F. Robey, J. O. Kane, B. A. Remington, R. P. Drake, O. A. Hurricane, H. Louis, R. J. Wallace, J. Knauer, P. Keiter, D. Arnett, and D. D. Ryutov, Physics of Plasmas **8**, 2446 (2001).

[25] A. R. Miles, D. G. Braun, M. J. Edwards, H. F. Robey, R. P. Drake, and D. R. Leibrandt, Phys. Plasmas **11**, 3631 (2004).

[26] R. Drake, D. Leibrandt, E. Harding, C. Kuranz, M. Blackburn, H. Robey, B. Remington, M. Edwards, A. Miles, T. Perry, *et al.*, Physics of Plasmas **11**, 2829 (2004).

[27] C. Kuranz, R. Drake, M. Grosskopf, A. Budde, C. Krauland, D. Marion, A. Visco, J. Ditmar, H. Robey, B. Remington, *et al.*, Physics of Plasmas **16**, 056310 (2009).

[28] E. Brambrinck, S. Baton, M. Koenig, R. Yurchak, N. Bidaut, B. Albertazzi, J. Cross, G. Gregori, A. Rigby, E. Falize, A. Pelka, F. Kroll, S. Pikuz, Y. Sakawa, N. Ozaki, C. C. Kuranz, M. Manuel, C. Li, P. Tzeferacos, and D. Lamb, HPLSE **4**, 31 (2016).

[29] N. C. Swisher, C. C. Kuranz, D. Arnett, O. Hurricane, B. A. Remington, R. H. F., and S. I. Abarzhi, PoP **22**, 102707 (2015).

[30] C. C. Kuranz, R. P. Drake, M. J. Grosskopf, B. Fryxell, A. Budde, J. S. Hansen, A. R. Mile, T. Plewa, N. Heam, and J. Knauer, PoP **17**, 052709 (2010).

[31] J. F. Hansen, H. F. Robey, R. I. Klein, and A. R. Miles, The Astrophysical Journal **662**, 379 (2007).

[32] A. Dubey, A. Almgren, J. Bell, M. Berzins, S. Brandt, G. Bryan, P. Colella, D. Graves, M. Lijewski, F. Lffler, B. O'Shea, E. Schnetter, B. Van Straalen, and K. Weide, Journal of Parallel and Distributed Computing **74**, 3217 (2014).

[33] B. Fryxell, K. Olson, P. Ricker, F. X. Timmes, M. Zingale, D. Q. Lamb, P. MacNeice, R. Rosner, J. W. Truran, and H. Tufo, Astrophysical Journal, Supplement **131**, 273 (2000).

[34] R. Yurchak, A. Ravasio, A. Pelka, S. Pikuz, E. Falize, T. Vinci, M. Koenig, B. Loupias, A. Benuzzi-Mounaix, M. Fatenejad, P. Tzeferacos, D. Q. Lamb, and E. G. Blackman, Phys. Rev. Lett. **112**, 155001 (2014).

[35] G. Dimonte, D. L. Youngs, A. Dimits, S. Weber, M. Marinak, S. Wunsch, C. Garasi, A. Robinson, M. J. Andrews, P. Ramaprabhu, A. C. Calder, B. Fryxell, J. Biello, L. Dursi, P. MacNeice, K. Olson, P. Ricker, R. Rosner, F. Timmes, H. Tufo, Y.-N. Young, and M. Zingale, Physics of Fluids **16**, 1668 (2004), https://doi.org/10.1063/1.1688328.

[36] A. Y. Faenov, T. A. Pikuz, P. Mabey, B. Albertazzi, T. Michel, G. Rigon, S. A. Pikuz, A. Buzmakov, S. Makarov, N. Ozaki, T. Matsuoka, K. Katagiri, K. Miyanishi, K. Takahashi, K. A. Tanaka, Y. Inubushi, T. Togashi, T. Yabuuchi, M. Yabashi, A. Casner, R. Kodama, and M. Koenig, Scientific Reports **8**, 16407 (2018).

[37] T. Pikuz, A. Faenov, N. Ozaki, T. Matsuoka, B. Albertazzi, N. Hartley, K. Miyanishi, K. Katagiri, S. Matsuyama, K. Yamauchi, H. Habara, Y. Inubushi, T. Togashi, H. Yumoto, H. Ohashi, Y. Tange, T. Yabuuchi, M. Yabashi, A. Grum-Grzhimailo, A. Casner, I. Skobelev, S. Makarov, S. Pikuz, G. Rigon, M. Koenig, K. Tanaka, T. Ishikawa, and R. Kodama, Matter and Radiation at Extremes (2018), https://doi.org/10.1016/j.mre.2018.01.006.

[38] A. Maiti, W. Small, J. Lewicki, T. Weisgraber, E. Duoss, S. Chinn, M. Pearson, C. Spadaccini, R. Maxwell, and T. Wilson, Scientific reports **6**, 24871 (2016).

[39] E. I. Moses, J. D. Lindl, M. L. Spaeth, R. W. Patterson, R. H. Sawicki, L. J. Atherton, P. A. Baisden, L. J. Lagin, D. W. Larson, B. J. MacGowan, G. H. Miller, D. C. Rardin, V. S. Roberts, B. M. V. Wonterghem, and P. J. Wegner, Fusion Science and Technology **69**, 1 (2016).

[40] A. Casner, T. Caillaud, S. Darbon, A. Duval, I. Thfouin, J. Jadaud, J. LeBreton, C. Reverdin, B. Rosse, R. Rosch, N. Blanchot, B. Villette, R. Wrobel, and J. Miquel, High Energy Density Physics **17, Part A**, 2 (2015), special Issue: 10th International Conference on High Energy Density Laboratory Astrophysics.

[41] N. Blanchot, G. Béhar, J. Chapuis, C. Chappuis, S. Chardavoine, J. Charrier, H. Coïc, C. Damiens-Dupont, J. Duthu, P. Garcia, J. P. Goossens, F. Granet, C. Grosset-Grange, P. Guerin, B. Hebrard, L. Hilsz, L. Lamaignere, T. Lacombe, E. Lavastre, T. Longhi, J. Luce, F. Macias, M. Mangeant, E. Mazataud, B. Minou, T. Morgaint, S. Noailles, J. Neauport, P. Patelli, E. Perrot-Minnot, C. Present, B. Remy, C. Rouyer, N. Santacreu, M. Sozet, D. Valla, and F. Laniesse, Opt. Express **25**, 16957 (2017).